Proc. Natl. Acad. Sci. USA
Vol. 92, pp. 2524–2528, March 1995
Ecology

Ecological chaos in the wake of invasion

JONATHAN A. SHERRATT*, MARK A. LEWIS†, AND ANDREW C. FOWLER‡

*Mathematics Institute, University of Warwick, Coventry CV4 7AL, United Kingdom; †Department of Mathematics, University of Utah, Salt Lake City, UT 84112; and ‡Mathematical Institute, 24-29 St. Giles', Oxford OX1 3LB, United Kingdom

Communicated by Robert M. May, University of Oxford, Oxford, United Kingdom, November 17, 1994

ABSTRACT **Irregularities in observed population densities have traditionally been attributed to discretization of the underlying dynamics. We propose an alternative explanation by demonstrating the evolution of spatiotemporal chaos in reaction–diffusion models for predator–prey interactions. The chaos is generated naturally in the wake of invasive waves of predators. We discuss in detail the mechanism by which the chaos is generated. By considering a mathematical caricature of the predator–prey models, we go on to explain the dynamical origin of the irregular behavior and to justify our assertion that the behavior we present is a genuine example of spatiotemporal chaos.**

The widespread spatial and temporal irregularities in actual population densities are in marked contrast to the smooth predictions of early ecological models (1–3). Simple ordinary differential equation models for three or more interacting species have long been known to exhibit chaotic behavior (4–6), but when only two species are involved, such simple models cannot predict chaos. Standard explanations for observed irregularities in such systems rely on discretization of space, time, or population density (7–9); difference equations, coupled oscillators, and cellular automata frequently exhibit chaotic solutions in appropriate parameter regimes. This raises the question of whether ecological chaos arising from interactions between two species depends intrinsically on discretization of population behavior. We present results suggesting that this is not the case. We show that spatiotemporal chaos can arise naturally in a class of reaction–diffusion models of predator–prey interactions. Necessary ingredients for this are classical oscillatory predator–prey dynamics (10, 11) plus random (diffusive) movement of both predators and prey. With these ingredients, a spatiotemporal invasion of predators may have chaotic solutions in its wake.

Chaotic solutions of reaction–diffusion equations are very rare and have previously been demonstrated, arising by quite different mechanisms, only in models of chemical reactions (12–16) and cardiac electrical activity (17, 18). Our work demonstrates chaos in ecological models of two interacting species without either discretization or delay effects.

Waves of Invasion

We consider reaction–diffusion models for predator–prey interactions of the form

$$\partial p/\partial t = D_p \partial^2 p/\partial x^2 + f_p(p, h) \qquad [1a]$$

$$\partial h/\partial t = D_h \partial^2 h/\partial x^2 + f_h(p, h). \qquad [1b]$$

Here $p(x, t)$ and $h(x, t)$ are the population densities of predators and prey with diffusion coefficients D_p and D_h, respectively, and x and t denote space and time. Throughout, we restrict attention to one-dimensional spatial domains. Biologically realistic kinetic terms f_p and f_h will have two nontrivial equilibria, a "prey only" state, in which $p = 0$, $h = h_0$, and a "coexistence" state, in which $p = p_s$, $h = h_s$. Models of type **1** have been studied by many previous authors in the case when $p = p_s$, $h = h_s$ is a stable equilibrium. In this case, one of the classical types of solution is a wave of invasion, that is, a traveling wave moving with constant shape and speed (19, 20). Ahead of the wave front there are prey but no predators ($p = 0$, $h = h_0$), and behind the wave the two species coexist ($p = p_s$, $h = h_s$). Standard linear analysis about the leading edge of the wave (19, 21) shows that the speed of invasion must be greater than $a = 2[D_p(\partial f_p/\partial p)|_{(p = 0,\ h = h_0)}]^{1/2}$ and numerical evidence, both for predator–prey models discussed here and for other equations of this type (21–23), suggests that invasive waves always travel at this minimum speed. Typically, a wave of this type arises when predators are introduced locally into an otherwise uniform distribution of prey.

We consider the analogue of these invasive waves when the kinetic parameters are such that $p = p_s$, $h = h_s$ is unstable, with the stable, spatially homogeneous, coexistence state consisting not of an equilibrium but of periodic temporal oscillations in p and h. Such stable limit cycles occur for many well-known kinetic terms (11), and to be specific, we consider two different sets that are both well-known as predator–prey models (24):

$$f_p(p, h) = Bp(1 - p/h)$$

$$f_h(p, h) = h(1 - h) - Ahp/(h + C) \qquad [2]$$

and

$$f_p(p, h) = Bp(A - 1 - Ae^{-Ch})$$

$$f_h(p, h) = h(1 - h) - p(1 - e^{-Ch}). \qquad [3]$$

In both sets of dynamics, A, B, and C are positive parameters, and for appropriate parameter values, the kinetics have a stable limit cycle. For a wide range of such parameters and for both sets of kinetics, we have studied numerically the evolution of model **1** following the local introduction of predators to an otherwise uniform distribution of prey. Intuitively, one might expect the solution to consist of an invasive wave front, with spatially homogeneous, temporal oscillations behind this. However, such solutions are never observed; rather, the behavior behind the wave front consists of either regular, spatiotemporal oscillations (Fig. 1*a*) or spatiotemporal oscillations that are irregular and apparently chaotic (Fig. 1*b*).

In the case of regular oscillations, detailed space–time plots show that these oscillations are periodic plane waves, moving with constant shape and speed (Fig. 2). These waves can move in either the same or the opposite direction to the invasive wave, depending on parameter values, but in all cases the wave speed is considerably greater than the speed of invasion. This difference in wave speed shows that the regular oscillations are not simply part of the invasive wave front; rather, they are a new type of solution that appears behind the invasive front as the coexistence steady state (p_s, h_s) becomes unstable, by means of a Hopf bifurcation in the kinetics. Now prior to Hopf

The publication costs of this article were defrayed in part by page charge payment. This article must therefore be hereby marked "*advertisement*" in accordance with 18 U.S.C. §1734 solely to indicate this fact.

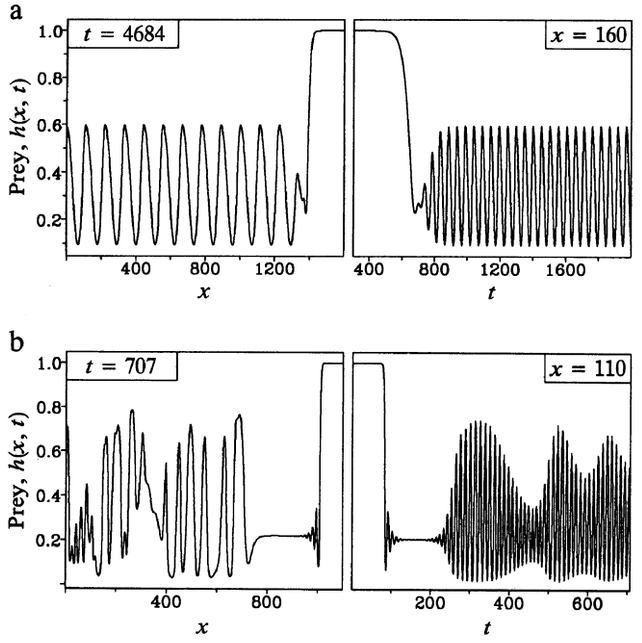

FIG. 1. Spatial and temporal variations in prey densities behind a wave of invasion by predators for a model whose kinetics have a stable limit cycle. The qualitative form of the predator distributions behind the invading front is very similar. (*a*) Invasion generates regular spatiotemporal oscillations in population densities. (*b*) Invasion generates highly irregular oscillations. The kinetics are from Eq. **3**, with $D_p = D_h = 1$; and $A = 1.5$. In *a*, $B = 0.05$ and $C = 4$, while in *b*, $B = 1$ and $C = 5$, and the equations were solved numerically by using the method of lines and Gear's method. In all the solutions in the figures, we take $D_p = D_h$; however, our mechanism applies equally to unequal dispersal rates.

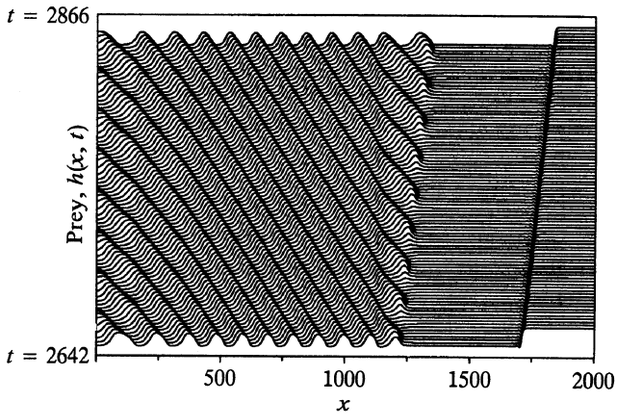

FIG. 2. Space–time plots of the prey density behind a wave of invasion by predators, for a model whose kinetics have a stable limit cycle and for parameter values giving regular oscillations behind the invading front. The qualitative form of the predator distributions behind the invading front is very similar. The oscillations move with constant shape and speed in the opposite direction to the invading wave; for some other parameters the oscillations move in the direction of invasion. The kinetics are from Eq. **2**, with $D_p = D_h = 1$; $A = 3$; $B = 0.1$; and $C = 0.2$. We plot the prey density $h(x, t)$ as a function of x at successive times, with the vertical separation of any two solutions proportional to the time interval between them.

bifurcation, the invasive front is a traveling wave solution satisfying the equations

$$D_p\hat{p}'' + a\hat{p}' + f_p(\hat{p}, \hat{h}) = 0 \qquad \textbf{[4a]}$$

$$D_h\hat{h}'' + a\hat{h}' + f_h(\hat{p}, \hat{h}) = 0 \qquad \textbf{[4b]}$$

$$\lim_{z\to\infty} \hat{p}(z) = 0, \qquad \lim_{z\to\infty} \hat{h}(z) = h_0,$$

$$\lim_{z\to-\infty} \hat{p}(z) = p_s, \qquad \lim_{z\to-\infty} \hat{h}(z) = h_s, \qquad \textbf{[4c]}$$

where prime denotes d/dz, $\hat{h}z = x - at$, and $p(x, t) = \hat{p}(z)$, $h(x, t) = \hat{h}(z)$. The difference between the oscillatory and invasive wave speeds suggests that this front solution persists after the Hopf bifurcation in the kinetics, and this is confirmed by numerical continuation of Eqs. **4**. The oscillatory wake arises because, although the invasive front persists, the steady state behind it is now unstable, and perturbations induced by the passage of the front itself are amplified by this instability. Moreover, it appears that the speed and direction of the regular oscillations are determined by the particular way in which the rear of the invasive front perturbs the steady state (p_s, h_s). It is known that in simpler reaction–diffusion systems, exponentially decaying perturbations applied to an unstable steady state can induce periodic plane waves whose speed varies continuously with the decay rate of the initial perturbation (25). In the present case, the rear of the invasive front does indeed decay exponentially to (p_s, h_s), at a rate given by the real part of the appropriate eigenvalue of Eqs. **4**. For a wide range of parameter values for which regular oscillations are observed, we have calculated this decay rate and imposed the corresponding perturbation on (p_s, h_s) in a simple numerical experiment. In each case, the perturbation induces periodic plane waves of the same speed as those observed behind the invasive fronts (Fig. 3).

We are now in a position to address the case of irregular wakes. In this case too, the rear of the invasive front will impose an exponentially decaying perturbation on (p_s, h_s), which will in turn give rise to periodic plane waves. The logical explanation for the appearance of irregular oscillations is that these periodic plane waves are unstable as reaction–diffusion solutions. This is confirmed by following the progression from regular to irregular wakes as one of the kinetic parameters is

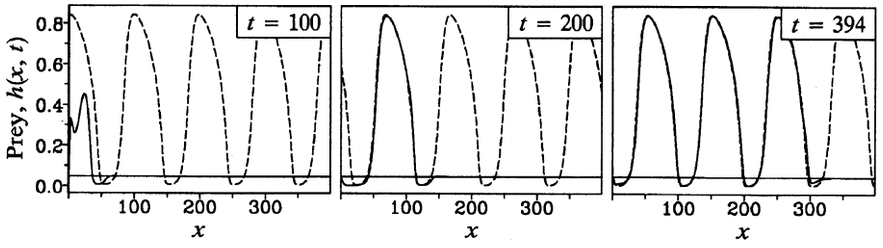

FIG. 3. Evolution of the solution of Eq. **1** following a small, exponentially decaying perturbation to the (unstable) coexistence steady state (p_s, h_s). The form of the perturbation has exactly the form of the tail of the invasive wave, so that the initial conditions are $[p(x, 0), h(x, 0)] = (p_s, h_s) + \varepsilon \cdot \mathrm{Re}[(p_e, h_e)\exp(-\lambda x)]$, where $\varepsilon \ll 1$, λ is the unstable eigenvalue of Eq. **4** at (p_s, h_s), which is unique up to complex conjugacy, and (p_e, h_e) is the corresponding normalized eigenvector. The prey density in the reaction–diffusion solution evolving from this initial condition is shown at three different times (—), and compares extremely well with the oscillations observed behind the invasive wave for the same parameters (- - -). In the latter solution, an appropriate spatial translation is applied at one time point to give correspondence between the two sets of solutions. A similarly good comparison is observed for the predator density and for other sets of parameter values. In the case illustrated, the kinetics are from Eq. **2**, with $D_p = D_h = 1$; $A = 3$; $B = C = 0.1$; and $\varepsilon = 0.005$.

varied. At the borderline between the two behaviors, the solution has a mixed appearance, with a band of regular oscillations immediately behind the invasive front, and irregular oscillations further back (Fig. 4). This behavior appears just as separate numerical tests (of the type illustrated in Fig. 3) show a transition to instability in the periodic plane waves induced by the rear of the invasive front. Thus, the mixed behavior occurs because the regular oscillations are only just unstable and persist transiently before the growth of instabilities gives rise to irregular behavior.

In our numerical studies, we have considered only two sets of kinetic terms. However, for both sets we have examined a wide range of parameter sets, and in all cases, the results are essentially the same. Moreover, we have presented a detailed explanation for the oscillatory wakes observed numerically; the mathematical details of the mechanism are described more fully elsewhere (23). This explanation depends only on the key ingredients of an invasive wave and kinetics with a stable limit cycle. Many predator–prey systems possess these ingredients, and, thus, we expect the phenomenon of irregular wakes to apply in many naturally occurring situations. Ideally, we would like to derive general conditions on f_p and f_h for the different types of behavior to occur, but this is prevented by the lack of general conditions for the stability of periodic plane waves as reaction–diffusion solutions, despite extensive mathematical study (26–28). Therefore, we can only derive parameter domains for regular and irregular wakes by using numerical simulations, and one such division of a cross section of parameter space is illustrated in Fig. 5.

The concept of spatiotemporal oscillations in the wake of invasion is not new in ecology. Jeltsch *et al.* (29) described data illustrating spatiotemporal oscillations behind waves of tephritid fly populations, which they explain by using a discrete-time model. Earlier data from the work of Caughley (30) on the Himalayan thar in New Zealand also illustrated oscillations behind invasion by a single species. On the theoretical side, Kot (31) has demonstrated period doubling cascades in the wake of invasive waves in integrodifference equations, and Kaneko (32) has studied chaos behind waves in systems of asymmetrically coupled logistic maps. However, the irregularities in these cases are a simple consequence of the local dynamics, rather than a new phenomenon introduced by dispersal. A different approach was taken in recent work by Pascual (33), who demonstrated chaos in diffusively coupled predator–prey systems of the form in Eqs. **1** but with a spatial variation in the prey growth rate. This is a fundamentally different mechanism from the one discussed here, because the chaos is induced externally by the imposed spatial variation, rather than arising naturally, as in the present study.

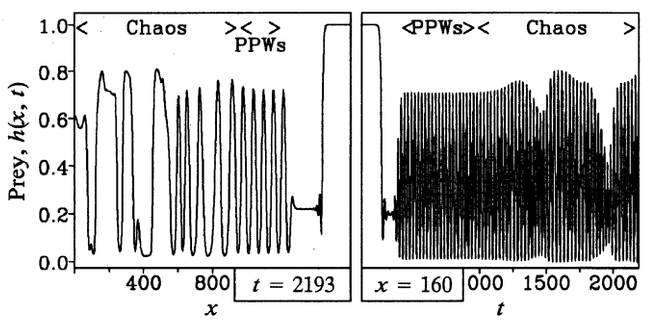

FIG. 4. Spatial and temporal variations in prey densities behind a wave of invasion by predators for parameters on the borderline between regular and irregular oscillations. The qualitative form of the predator distributions behind the invading front is very similar. Immediately behind the invading front, there are regular spatiotemporal oscillations, corresponding to periodic plane waves (PPWs). However, these periodic plane waves are just unstable, and further back from the front, instabilities have had time to grow, giving rise to irregular behavior. The kinetics are from Eq. **3**, with $D_p = D_h = 1$; $A = 1.5$; $B = 0.22$; and $C = 5$.

The Route to Chaos

A key outstanding question concerns the nature of the irregular oscillations discussed above: is this really an example of spatiotemporal chaos or just behavior that appears irregular on superficial inspection but in reality has underlying order? Routes to chaos in spatially discrete models are well known, enabling this question to be answered relatively easily, but the spatially continuous case is much less well understood. Therefore, in order to simplify matters as much as possible, we will consider a mathematical caricature of the rather complex predator–prey models discussed above. Specifically, we will focus on a reaction–diffusion equation of λ–ω type,

$$\partial u/\partial t = \partial^2 u/\partial x^2 + (1 - r^2)u - (3 - r^2)v \qquad \textbf{[5a]}$$

$$\partial v/\partial t = \partial^2 v/\partial x^2 + (3 - r^2)u + (1 - r^2)v \qquad \textbf{[5b]}$$

where $r = (u^2 + v^2)^{1/2}$. The choice of this particular λ–ω system is essentially arbitrary. The system has kinetics with a (circular) stable limit cycle and a unique (unstable) steady state at the origin, and it is, thus, unable to reflect the phenomenon of invasive waves. However, the limit cycle means that the equations do possess periodic plane waves, and exponentially decaying perturbations to the $u = v = 0$ equilibrium again induce periodic plane waves. The main advantage of a λ–ω system is that the form and stability of periodic plane wave solutions can be determined analytically: the waves are $r = R$, $\theta = (3 - R^2)t \pm (1 - R^2)^{1/2}x$, where (r, θ) are polar coordinates in the u–v plane, and the amplitude $R \in (0, 1)$ parameterizes the wave family (26). This solution is stable on $0 < x < L$ whenever $R > R_{crit}$, a critical value that depends on the domain length L and the boundary conditions. This detailed knowledge of the form and stability of periodic plane waves makes it much simpler to investigate the behavior resulting from the perturbation of unstable periodic plane waves; however, we

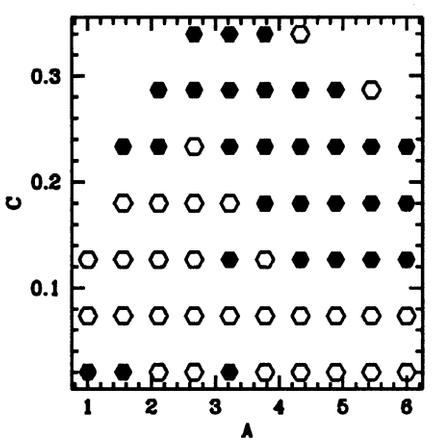

FIG. 5. Example of the division of parameter space into regions giving regular and irregular wakes. The cross-section $B = 0.1$ of the three-dimensional A–B–C parameter space is shown with open hexagons indicating a regular wake and filled hexagons indicating an irregular wake. The distinction between the two cases was made by numerical determination of the growth or decay of localized perturbations in the wake region. Specifically, Eqs. **1** were solved numerically up to $t = t_1$, and then the solution was continued up to $t = t_2$ for two sets of the equations in parallel and in one case with a small perturbation applied at $x = x_{pert}$. The differences between the two solutions were used to determine whether the initial perturbation had grown or decayed, corresponding to an irregular or regular wake, respectively. In fact, the procedure was carried out for a number of values of t_1, t_2 and in particular x_{pert}, since for some parameter values the growth of the perturbation is only evident in the time interval we are considering in some parts of the wake region.

anticipate that the key aspects of our results will also hold for the predator–prey models. Our use of λ–ω systems as a mathematical caricature of more general reaction–diffusion models follows similar approaches by many previous authors, most notably in the study of spiral waves (34, 35).

We have solved the Eqs. **5** numerically on $0 < x < L$, $t > 0$, with the initial solution at $t = 0$ given by a small random perturbation of the periodic plane wave of amplitude R. In order that the boundaries do not force instability, we require boundary conditions at $x = 0$ and $x = L$ that will be satisfied by the periodic plane wave. One possibility is periodic boundary conditions, but this would require the domain length to be a whole number of wavelengths, and thus to vary with R. To avoid this restriction, we impose instead $\partial r/\partial x = 0$ and $\partial\theta/\partial x = (1 - R^2)^{1/2}$ at the boundaries. For given values of L, we have studied in detail the variation with R of the long-term behavior in numerical solutions of Eqs. **5.** The results are most conveniently described in terms of the spatial and temporal behavior of the solution amplitude r, recalling that the periodic plane wave solution has $r = R$, constant. For sufficiently large values of L, spatiotemporal irregularities are observed in these finite domain solutions, and we will discuss the sequence of behaviors for $L = 30$ in detail. The solution for R just below $R_{crit} \approx 0.809$ consists of small, decaying oscillations in r. However, as R is decreased, there are two intervals of R values for which the long-term solution exhibits spatiotemporal irregularities. Our numerical observations suggest that these irregularities arise through bifurcation sequences that are well known from ordinary differential equations, namely periodic doubling and bifurcations to tori (Table 1).

Two aspects of these results are relevant to the present study. First, the appearance of these well known routes to chaos is a very strong indication that the irregular behavior is genuinely chaotic in time. In addition, it is clear that the initial periodic plane wave amplitude R is a key bifurcation parameter. Now, R enters our scheme in two separate ways: in the boundary conditions and in the initial conditions. To consider which of these is the crucial effect, we fixed R at a value giving chaotic behavior and varied separately the initial and boundary conditions. This showed very clearly that the rich structure described in Table 1 depends on the boundary conditions we are using and is essentially independent of the initial solution. How does this relate to the chaotic wakes we have described in predator–prey models? We have shown that the passage of the invasive front perturbs the (unstable) coexistence steady state in a way that induces periodic plane waves. Now the front is, by definition, always at the boundary of the wake region; of course, this is a moving boundary, and moreover there is a boundary of this type at only one edge of the wake region. With this proviso, the front induces a boundary condition on the wake of exactly the type we have imposed in our bifurcation study, and thus the λ–ω study strongly suggests that it is this boundary effect that generates the chaotic wake.

Table 1. Long-term behavior of Eqs. **5** as R varies for L = 30

R range (approx.)	Long-term behavior of $r(x, t)$
$1 > R > 0.809$	$r = R$ (periodic plane wave)
$0.809 > R > 0.807$	Regular spatiotemporal oscillations, periodic in time, decaying with x
$0.807 > R > 0.805$	Period doubling cascade in temporal behavior, synchronously in space
$0.805 > R > 0.79$	Spatiotemporal chaos
$0.79 > R > 0.545$	Regular spatiotemporal oscillations These appear from the chaotic behavior in a sharp transition
$0.545 > R > 0.52$	The temporal behavior bifurcates to a torus and, thence, to chaos. This occurs via a "wave of bifurcation" in x
$0.52 > R > 0.45$	Spatiotemporal chaos
$0.45 > R > 0.4$	The temporal behavior undergoes a reverse bifurcation sequence, via a torus, to periodic oscillations
$0.4 > R > 0$	Regular spatiotemporal oscillations

The initial and boundary conditions are as discussed in the text.

The hallmark of a chaotic solution is that small perturbations grow to induce large scale differences in the solution, and this is indeed the case in the irregular wakes (Fig. 6). Not only does a locally applied perturbation grow in time, but it also propagates spatially through the wake region. It is this spatial propagation of instability that leads us to describe the solution as spatiotemporal chaos. Our analysis thus suggests that spatiotemporal chaos in predator–prey systems is not limited to the dynamics given in Eqs. **2** and **3.** We conjecture that, when diffusive terms have been added to the predator and prey dynamics, the classical rules given by Kolmogorov (10) to ensure predator–prey oscillations may, in turn, ensure chaotic solutions after an invasion of predators.

It is well known that diffusion can destabilize the spatially homogeneous steady-state solution (p_s, h_s) and lead to diffusion-driven instabilities and eventually to clumping of the predator and prey populations (see ref. 36 for a review). Our analysis indicates a way in which diffusion can destabilize predator–prey dynamics: addition of diffusion to predator–prey oscillations can lead to irregular fluctuations in both predator and prey densities and eventually to spatiotemporal chaos. An indication that this may be a general property of oscillatory predator–prey interactions rather than an artifact of reaction–diffusion models is provided by our observations of similar behavior in spatially and temporally discrete models for predator–prey interactions (Fig. 7). This underscores the message that, in ecology, random movement, as modeled by

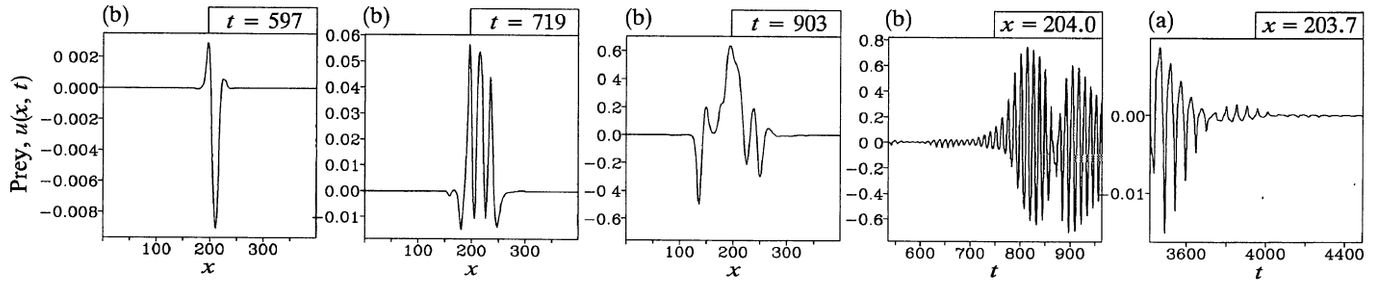

FIG. 6. Development of a small, localized perturbation applied to the wake region. Eqs. **1** were solved numerically up to a fixed time, and then the solution was continued for two sets of the equations in parallel, in one case with a small perturbation applied in the wake region. Specifically, 1% of the steady-state values was added to u and v in the region $200 < x < 210$. The figure shows the difference between the two solutions for prey density u—i.e., the development of the perturbation; the solution for the predator density is very similar. The kinetics are from Eq. **2**, with parameter values as in the legend to Fig. 1; thus *a* corresponds to a regular wake and the perturbation rapidly decays, while in *b*, corresponding to an irregular wake, the perturbation grows and expands in space. In both cases, the way in which the perturbation develops is not sensitive to details such as when or where within the wake region it is applied.

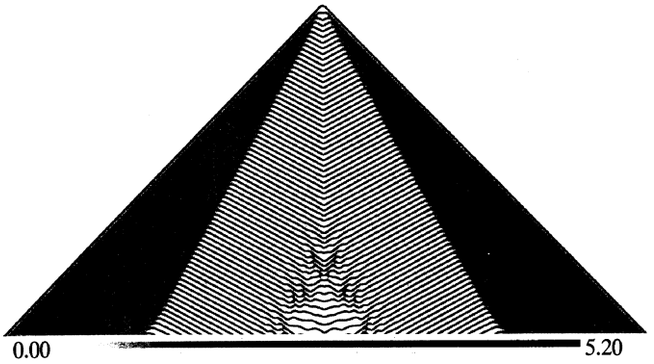

FIG. 7. Solution illustrating the formation of periodic waves and an irregular wake behind invasion in a discrete space and discrete time model for predator–prey interaction. The predator density is illustrated using the grey scale indicated; the solution for the prey density has a qualitatively similar form. The solution is illustrated as a space–time plot: the discrete spatial patches are represented by pixels running across the page, with successive time steps running down the page. The discretization is barely visible at this magnification. The model equations are taken from ref. 37, with parameter values $r = 1.2$; $a = 1$; $K = 8$; and $\alpha = 1$ (notation as in ref. 37). The model in ref. 37 is a temporal difference equation, and to incorporate spatial effects, the predator and prey densities are replaced at the end of each iteration by a weighted average of the density at the current patch and the two neighboring patches; for the solution shown the weighting is 0.05:0.425:0.425. The solution is shown for 498 time steps on a spatial domain of 1001 patches; initially there are no predators and a steady-state density of prey in each patch, except patch number 501, in which a predator density of 0.01 is introduced. This system has no formal mathematical relationship with the reaction–diffusion systems considered previously, although it is modeling a similar biological situation, and the occurrence of the same phenomena of regular and irregular wakes in the two types of model strongly supports the possibility that this is a real biological phenomenon rather than a modeling artifact.

diffusion, cannot be considered merely as a spatial averaging process; in the system here, diffusion heralds the onset of irregular, unpredictable fluctuations, which cannot be explained by the underlying growth dynamics.

J.A.S. was supported in part by grants from the Royal Society of London and the Nuffield Foundation. M.A.L. was supported in part by a grant from the National Science Foundation (DMS-9222533).

1. Verhulst, P. F. (1838) *Corr. Math. Phys.* **10,** 113–121.
2. Lotka, A. J. (1920) *J. Am. Chem. Soc.* **42,** 1595–1599.
3. Volterra, V. (1926) *Memorie Academei dei Lincei* **2,** 31–113.
4. Gilpin, M. E. (1979) *Am. Nat.* **113,** 306–308.
5. Schaffer, W. M. (1985) *IMA J. Math. Appl. Med. Biol.* **2,** 221–252.
6. Kot, M., Sayler, G. & Schultz, T. (1992) *Bull. Math. Biol.* **54,** 619–648.
7. May, R. M. (1986) *Proc. R. Soc. London B* **228,** 241–266.
8. Hassell, M. P., Comins, H. N. & May, R. M. (1991) *Nature (London)* **353,** 255–258.
9. Comins, H. N., Hassell, M. P. & May, R. M. (1992) *J. Anim. Ecol.* **61,** 735–748.
10. Kolmogorov, A. N. (1936) *G. Ist. Ital. Attuari* **7,** 74–80.
11. May, R. M. (1981) *Stability and Complexity in Model Ecosystems* (Princeton Univ. Press, Princeton, NJ).
12. Kuramoto, Y. (1978) *Prog. Theor. Phys.* **64,** 346–367.
13. Kuramoto, Y. & Koga, S. (1981) *Prog. Theor. Phys.* **66,** 1081–1085.
14. Kuramoto, Y. (1984) *Chemical Oscillations, Waves and Turbulence* (Springer, Berlin).
15. Nandapurkar, P. J., Hlavacek, V. & Van Rompay, P. (1986) *Chem. Eng. Sci.* **41,** 2747–2760.
16. Rovinsky, A. B. (1987) *J. Phys. Chem.* **91,** 5113–5118.
17. Fishler, M. G. & Thakor, N. V. (1991) *Pacing Clin. Electrophysiol.* **14,** 1694–1699.
18. Courtemanche, M. & Winfree, A. T. (1991) *Int. J. Bifurcation Chaos* **1,** 431–444.
19. Dunbar, S. R. (1983) *J. Math. Biol.* **17,** 11–32.
20. Dunbar, S. R. (1984) *Trans. Am. Math. Soc.* **268,** 557–594.
21. Sherratt, J. A. (1994) *SIAM J. Appl. Math.* **54,** 1374–1385.
22. Dale, P. D., Sherratt, J. A. & Maini, P. K. (1994) *Appl. Math. Lett.* **7,** 11–14.
23. Sherratt, J. A. (1994) *Physica D* **70,** 370–382.
24. Murray, J. D. (1989) *Mathematical Biology* (Springer, Berlin).
25. Sherratt, J. A. (1993) *Nonlinearity* **6,** 1055–1066.
26. Kopell, N. & Howard, L. N. (1973) *Stud. Appl. Math.* **52,** 291–328.
27. Othmer, H. G. (1977) *Lect. Math. Life Sci.* **9,** 57–86.
28. Maginu, K. (1981) *J. Differ. Equ.* **39,** 73–99.
29. Jeltsch, F., Wissell, C. H., Eber, S. & Brandel, R. (1992) *Ecol. Modell.* **60,** 63–75.
30. Caughley, G. (1970) *Ecology* **51,** 53–72.
31. Kot, M. (1992) *J. Math. Biol.* **30,** 413–436.
32. Kaneko, K. (1985) *Phys. Lett.* **111,** 321–325.
33. Pascual, M. (1993) *Proc. R. Soc. London B* **251,** 1–7.
34. Greenberg, J. M. (1980) *SIAM J. Appl. Math.* **39,** 301–309.
35. Koga, S. (1982) *Prog. Theor. Phys.* **67,** 164–178.
36. Okubo, A. (1980) *Diffusion and Ecological Problems: Mathematical Models* (Springer, Berlin).
37. Beddington, J. R., Free, C. A. & Lawton, J. H. (1975) *Nature (London)* **255,** 58–60.